EUROPEAN
MATERIALS RESEARCH SOCIETY

Strasbourg (France)

MANUSCRIPT COVER PAGE FORM

E-MRS Symposium **: B**

Paper Number **: # 2007**

Title of Paper **: COMPREHENSIVE, PHYSICALLY BASED MODELLING OF As IN Si**

Corresponding Author **:** R. Pinacho

Full Mailing Address **: Dto de Electronica**
E.T.S.I. de Telecomunicacion. Campus Universitario Miguel Delibes
47011 VALLADOLID
ESPAÑA

Telephone **: 983 42 36 83 (ext. 5505)**

Fax **: 983 42 36 75**

E-mail **: rutpin@tel.uva.es**

COMPREHENSIVE, PHYSICALLY BASED MODELLING OF As IN Si

R. Pinacho, M. Jaraiz, P. Castrillo, J. E. Rubio, I. Martin-Bragado, J. Barbolla, Dpt. of Electronics, University of Valladolid, 47011 Valladolid, Spain

An accurate knowledge of the behavior of Arsenic appearing at high concentrations during thermal processes is essential for today's CMOS technology so that As is the most widely used n-type Si dopant in ultralarge scale integrated circuits. In spite of the large amount of successful research work devoted to reproducing As kinetics in Si, the level of complexity reached by Si device fabrication technologies claims for a more comprehensive physical modeling that, based on fundamental parameters of some basic As configurations could simultaneously account for aspects such as diffusion, electrical deactivation and amorphization/ recrystallization after As implantation and annealing among others.

We have used the atomistic kinetic Monte-Carlo simulator DADOS to develop a consistent physical model for As that includes a limited set of AsV clusters of different sizes and energies. Through a detailed modeling of Fermi level effects, we will discuss the main features of As behavior in Si such as (i) intrinsic and extrinsic As diffusion, (ii) electrical deactivation at high As concentrations, (iii) annealing of As implanted profiles and (iv) other striking features such as the interstitial supersaturation induced by rapid electrical deactivation of very high As concentrations at low temperatures.

Finally, in order to test the model, this has been implemented with DADOS and compared with experiments, showing a good agreement in all the cases.

INTRODUCTION

Arsenic is the most widely used n-type dopant in Silicon due mainly to its low diffusivity and high electrical activation level, both crucial properties when it comes to maximizing the conductivity of ever shallower device junctions. Thanks to nonequilibrium processing methods such as laser annealing and ion implantation followed by rapid thermal annealing, specimens with very shallow and high As concentrations, even above its solubility, can be fabricated. In such a regime, simulation models to reproduce As behavior must include several high concentration effects taking place simultaneously during the process steps. Among them, besides the extrinsic diffusion [1], which occurs at As concentrations higher than the intrinsic electron concentration n_i, the most singular feature is that As undergoes a rapid electrical deactivation during annealing in the regions treated by laser-melt annealing [2] or by amorphizing As implants [3]. In addition to this effect, a comprehensive model to describe Si amorphization and recrystallization is also necessary since the heavy As atom can easily amorphize Si for common typical processing conditions.

Kinetic Monte-Carlo simulators seem to be ideal to reproduce these experiments since they can include as many reactions as necessary without the penalty of increased computation time. Besides, the parameters used are directly related to calculated physical models for the different As configurations and intrinsic and extended defects in Si. The atomistic kinetic Monte-Carlo simulator DADOS [4] has proven to be able to reproduce and accurately predict the formation and eventual dissolution of defects that appear simultaneously in non-equilibrium conditions such as {311}'s, dislocation loops as well as the amorphization and recrystallization of implanted layers [5]. In this work, we incorporate a comprehensive model for As in Si that with a reduced set of AsV cluster parameters into the DADOS simulator, can account for the above mentioned experimental features while being also consistent with first-principles calculations and the previously implemented DADOS models for the rest of the Si phenomena taking place during the different process steps.

THE MODEL

Due to the special diffusion features of As, new processes had to be included into DADOS. The model can be categorized into three main points: (i) Extrinsic As diffusion is assisted by both, vacancy and interstitialcy mechanisms, (ii) As electrical deactivation is mediated by the formation of As_nV_m clusters, (iii) this electrical deactivation is very fast in its initial stages when there is a high As concentration layer created either by a superficial laser-melt annealing or by the recrystallization process of the amorphous layer generated during As implantation. In the following, we will explain each of the three issues:

(i) Although there are some inconsistencies in the experiments [1], As seems to diffuse via vacancy (ring) and interstitialcy (kick-out) mechanisms [6]. Therefore, As diffusion in Si can be written as:

$$D_{As}^{*} = D_{AsV}^{*} + D_{Asi}^{*} \qquad (1)$$

where D_{As}^{*} is the As diffusivity in equilibrium conditions and D_{AsV}^{*}, D_{Asi}^{*} the fractions due to the vacancy and the interstialcy mechanisms, respectively. From the atomistic point of view, the two contributions are the consequence of the existence of two mobile As configurations, which we call AsV and Asi, while the substitutional As (As_s) can be considered immobile and electrically active. AsV is the association of an As atom with a vacancy (V) while Asi denotes either an As in an interstitial position or a pair of a substitutional As plus a self-interstitial (I). The reactions that control As diffusion are then:

$$\begin{aligned} As_s + V &\leftrightarrow AsV \\ As_s + I &\leftrightarrow Asi \end{aligned} \qquad (2)$$

The migration and binding energies of AsV and Asi determine the As diffusion. If the concentrations of AsV and Asi are altered, e.g., due to the I supersaturation generated after As implantation, the As experiences transient enhanced diffusion (TED). The effective As diffusivity can also vary when there is a high electrically active As concentration, well above

the intrinsic electron concentration n_i at the annealing temperature. In this case, the As diffusion occurs under extrinsic doping conditions. Since the mobile As configurations have energy states in the bandgap, they can either trap or release electrons, appearing in different charge states as AsV^0, AsV^-, AsV^+, Asi^0 and Asi^+ and alter their concentrations according to the position of the Fermi level in the bandgap, that is, according to the dopant concentration at each point of the material. Consequently, in these conditions the As diffusivity D_{As} depends on the electrically active As concentration as it has been reported in many works [7]. Table I summarizes the migration and binding energies of the mobile species involved in As diffusion as well as their position in the bandgap. The values of migration and binding energies of AsV^0 are from first-principles calculations [8]. Regarding Asi, we have found in the literature much more controversy about its energies estimates [9, 10]. Therefore, the energy values of Asi have been chosen to fit the total intrinsic As diffusion to the form:

$$D^*_{As} = D^*_{AsV} + D^*_{Asi} = 14.5\exp(-4.05/kT)\ cm^2/s \qquad (3)$$

that is used in the TSupremIV [11].

Using the parameters on Table I, a good agreement can be achieved between the continuum differential equation-based model for As extrinsic diffusion and the atomistic simulation performed with DADOS for different values of the n/n_i rate [12].

Figure 1 shows a comparison between the concentration-dependent As diffusivity predicted by DADOS and the experimental results from Fair [7]. The extrinsic As diffusion [1] can be described with the equation:

$$D_{As} = D_{AsV} + D_{Asi} = h\left[D^i_{AsV^+} + D^i_{AsV^0}\frac{n}{n_i} + D^i_{AsV^-}\left(\frac{n}{n_i}\right)^2 + D^i_{Asi^+} + D^i_{Asi^0}\frac{n}{n_i} \right] \qquad (4)$$

where D^i_X is the diffusivity of the X species in intrinsic conditions, n the electron concentration, n_i the intrinsic electron concentration and h the electric field factor [1]. With the parameters given in Table 1, the diffusion is mainly carried out via AsV^0 which leads to the predominance of the second term in Eq. (4) and therefore predicts a linear dependence of

As diffusivity with the electron concentration. Using Maxwell-Boltzmann statistics, n can be written as:

$$n = \frac{[As_s]}{2} + \left(\frac{[As_s^2]}{4} + n_i^2 \right)^{1/2} \quad (5)$$

then, at high As concentration conditions ($[As_s] >> n_i$), the DADOS model predicts an almost linear As diffusion dependence on As concentration. This is the range shown in Figure 1, in good agreement with experiments.

(ii) At high As concentrations, above $\approx 3x10^{20} cm^{-3}$, electrical As deactivation happening simultaneously to As diffusion is a phenomenon clearly observed [3]. This process presents a remarkable amplitude. In fact, the maximum concentration limit of dissolved As in equilibrium with its precipitates, exceeds by one order of magnitude the value of the carrier concentration limit [13, 14]. Clustering of the dissolved As atoms is commonly accepted as the phenomenon responsible for the electrically inactive, unprecipitated dopant in Si. Different cluster models have been proposed. All of them assume the formation of aggregates, electrically inactive at room temperature, consisting of a fixed number of dopant atoms in specific lattice configurations which can include vacancies or even interstitials [2, 8, 15 ,16, 17, 18]. The proposed models range from aggregation of two dopant atoms, without associated vacancies [18] to clusters consisting of two to four dopant atoms including vacancies or interstitials [2, 8, 15, 16, 17]. However, recent experiments (Hall and resistivity measurements, positron annihilation) clearly favor a deactivation mechanism induced by As_nV clustering [19, 20]. These clusters must be energetically favored in comparison with the substitutional electrically active As, due to their low formation energies and then, after the thermal treatment most of the As atoms remain in such stable configurations.

In our model, we have included the formation of electrically neutral As_nV_m clusters, which are agglomerates formed by As atoms and Vacancies. We have not included clusters of As combined with self-interstitials, As_nI_m because according to most part of calculations, they do

not seem to be stable enough [8, 15-16]. In Table II the total binding energies of As clusters are summarized. As can been clearly seen, As_2V, As_3V, As_4V are the most stable clusters, in good agreement with most first-principles calculations [8, 15-17] and recent experimental observations [19, 20].

The kinetics of As deactivation is controlled by the growth/shrinkage of the As_nV_m clusters. Taking into account that in the As case there are two mobile species (AsV and Asi) the diffusion-assisted growth/shrinkage is described by the following reactions in the forward/reverse direction:

$$As_nV_m + V \leftrightarrow As_nV_{m+1} \qquad \text{trapping/emission of a V} \qquad (6)$$

$$As_nV_m + AsV \leftrightarrow As_{n+1}V_{m+1} \qquad \text{trapping/emission of an AsV} \qquad (7)$$

$$As_nV_m + I \leftrightarrow As_nV_{m-1} \qquad \text{trapping/emission of an I} \qquad (8)$$

$$As_nV_m + Asi \leftrightarrow As_{n+1}V_{m-1} \qquad \text{trapping/emission of an Asi} \qquad (9)$$

On the other hand, notice that the reverse reaction of the last two expressions conveys the formation of an I-V pair from the bulk. The Vacancy remains immobilized in the clusters while the interstitial is emitted alone (Eq. (8)) or combined with an As (Eq.(9)). In consequence, in both cases, an anomalous enhanced As diffusion can be generated.

(iii) So far we have explained how As diffuses (i) and how the As_nV_m clusters can grow and dissolve (ii). However, we have not explained yet how the As clusters appear in the first place. For high active As concentrations ($2.3x10^{20}$-$1.9x10^{21}$) grown upon recrystallization of laser-melt As doped layers, it has been experimentally observed that the initial electrical deactivation is very rapid (within 15 seconds) even at low temperature (down to 500ºC) [2, 21]. Besides, interstitials are injected into the substrate. At such a low temperature, the thermal surface-generated V and I concentrations are very low and therefore, the diffusion-assisted formation of the clusters originated by them would be much slower than is experimentally observed. Then, in order to explain such a rapid deactivation, some works [2] propose the bulk formation of As_nV associated with an I emission, according to Eq. (8).

On the other hand, a similar effect can be observed in implanted and rapidly recrystallized high As concentration layers. In this case, although no defects are supposed to remain in the bulk recrystallized layer, there is only a fraction of electrically active As, its upper limit being around $1x10^{21}$ cm^{-3} [3].

In the DADOS simulator, both phenomena are properly reproduced by the reverse reaction of Eq. (8). In fact, with the energies given in Table II, the bulk formation of As_2V, As_3V, and As_4V is quite fast, even at low temperatures, by reactions like:

$As + As + As \rightarrow As_3V + I$. For these processes to take place it is necessary that the As concentration is high enough to exist a high probability of two, three or four As atoms to be placed close to each other and therefore to transform into the As_nV cluster by the ejection of an I. Thus, this process is highly dependent on As concentration, as experimentally observed [2].

RESULTS AND DISCUSSION

In order to test our model, we have simulated the experiments performed by Rousseau et al. [2]. The experimental structures consist of a buried Boron layer as an interstitial detector, and a fully activated As doped laser annealed surface layer with a high concentration, $4.5x10^{20}$ cm^{-3} as shown in Figure 2. During a 750ºC annealing the As deactivates while the B suffers an enhanced diffusion due to the interstitial generation.

In Figure 2, Rousseau experimental data [2] and DADOS simulations are compared. As it can be seen, a good fit is achieved. DADOS simulation indicates that, in the first few seconds of annealing, the dominant cluster composition is As_2V. This is due to the higher probability of only two As to be close enough to each other to convert into As_2V in comparison with three or four As atoms. The I's generated during As_2V, As_3V, and As_4V formation diffuse and eventually combine with isolate substitutional As atoms creating Asi's. These Asi's increase As diffusion and make the clusters grow according to the forward reaction of Eq. (9) and the

reverse reaction of Eq. (8). At the end of the annealing, most part of the inactive As remains as As_3V, in good agreement with Lawther et al. [20] who have found by positron annihilation experiments that the average number of As atoms surrounding a vacancy are 2.5 and 3.2 for annealing times of 15 s and 2 h at 750ºC, respectively. A fraction of As is in the form of As_4V_2 that can be formed from As_3V by Eq. (7) or from As_4V by Eq. (8). Also, it is clear from Figure 2 that the measured B diffusion, and consequently the I supersaturation, is accurately predicted by our model. Finally, in figure 3, DADOS results about I agglomerates formation are shown. As can be clearly seen, the DADOS simulation predicts the formation of dislocations loops since the very beginning of the thermal treatment in good agreement with experiments [22].

We have also simulated some experiments of amorphizing As implants and subsequent annealing in order to check the prediction of the amorphized layer and the behavior of the above As diffusion/clustering model upon recrystallization [5].

In Figure 4 a), b) the experiments of Kim et. al [23] with 30 keV As amorphizing implants and subsequent annealing at 720ºC and 820ºC respectively together with DADOS simulations are displayed. A good agreement between experiments and simulations is again achieved. DADOS simulation shows that the amorphous layer created during the implant, which extends as far as 50 nm depth, is rapidly recrystallized within the first few seconds of the thermal treatment. After this, in the regrown region a small fraction of As is in the form of the energetically favorable As_nV clusters. This fraction grows slightly during annealing due to cluster ripening. At both temperatures, As exhibits TED due to the Asi diffusion that is increased by the I supersaturation created by the implant. Finally, as it is shown in figure 5 for the 720ºC annealing, the {311}'s evolve into dislocation loops appearing beyond the a/c interface, trapping the I excess and slowing down the As anomalous diffusion at longer times.

CONCLUSIONS

A comprehensive physical model has been developed to explain As behavior in Si. Emphasis has been put in including high concentration effects such as extrinsic diffusion and electrical deactivation. With such a model, the experiments of rapid electrical deactivation of high active As concentrations laser-melt layers and the amorphizing implanted and subsequently recrystallized As profiles can be accurately reproduced.

This work has been partially supported by the Spanish Government under project BFM2001-2250 and by the Castilla y Leon regional Government under project VA-010/02

Table I. As diffusion parameters for the mobile As species included in DADOS. The superscript denotes the charge state of the defect. Diffusivities relate to the general form $D_X = D_0 \exp(-E_m/kT)$ cm^2/s. The deep level in the band-gap is supposed to vary proportionally to the temperature band gap narrowing. The binding energy of the species depends on temperature due to the same effect [12].

Defect	D_0 (cm^2/s)	E_m (eV)	E_b (eV) T=0 K	e_t-e_V (eV) T=0 K
AsV^0	$1x10^{-3}$	1.4 [ref. 8]	1.3 [ref. 8]	
AsV^+	$1x10^{-3}$	1.4	1	0.3
AsV^-	$1x10^{-3}$	1.7	1.6	0.77 [ref. 1]
Asi^0	$2x10^{-3}$	1.7	1.4	
Asi^+	$2x10^{-3}$	1.7	0.5	0.1

Table II. Total binding energies of the As_nV_m clusters. Note that due to their low energy, As_2V, As_3V and As_4V can be formed in the bulk when the As atoms are close enough (i.e. $As + As + As \rightarrow As_3V + I$), that is, at high As concentrations.

As 0	As_2 0	As_3 0	As_4 0
	As_2V -5	As_3V -6	As_4V -6
			As_4V_2 -10.3

Figure 1. – As diffusivity versus total As concentration for different temperatures. Symbols are from experimental results [7], lines are the values predicted by DADOS.

Figure 2. – SIMS data of the structures utilized in the experiment of Rousseau et al. [2] consisting of a buried B layer and a superficial As layer implanted and laser-melt annealed. After 750ºC 2 h annealing, SIMS data show large enhanced diffusion of the buried B layer. DADOS simulation (lines) fits well the As and B profiles. Note that DADOS simulation predicts an electrically active As concentration around $2x10^{20}$ cm^{-3} in good agreement with experiments [2].

Figure 3. – I agglomerates evolution during the experiment of figure 2 (Rousseau et al.) predicted by DADOS. Note the formation of dislocation loops in good agreement with ref. 22

Figure 4. – SIMS As profiles from Kim et al. [23] for samples implanted with 30 keV, $5x10^{14}$ cm^{-2} As and subsequently annealed at two different temperatures: a) 720 ºC for 300 min and b) 820 ºC for 1 and 30 min, together with DADOS simulations.

Figure 5. – I agglomerates evolution during the experiment of figure 4 a) predicted by DADOS

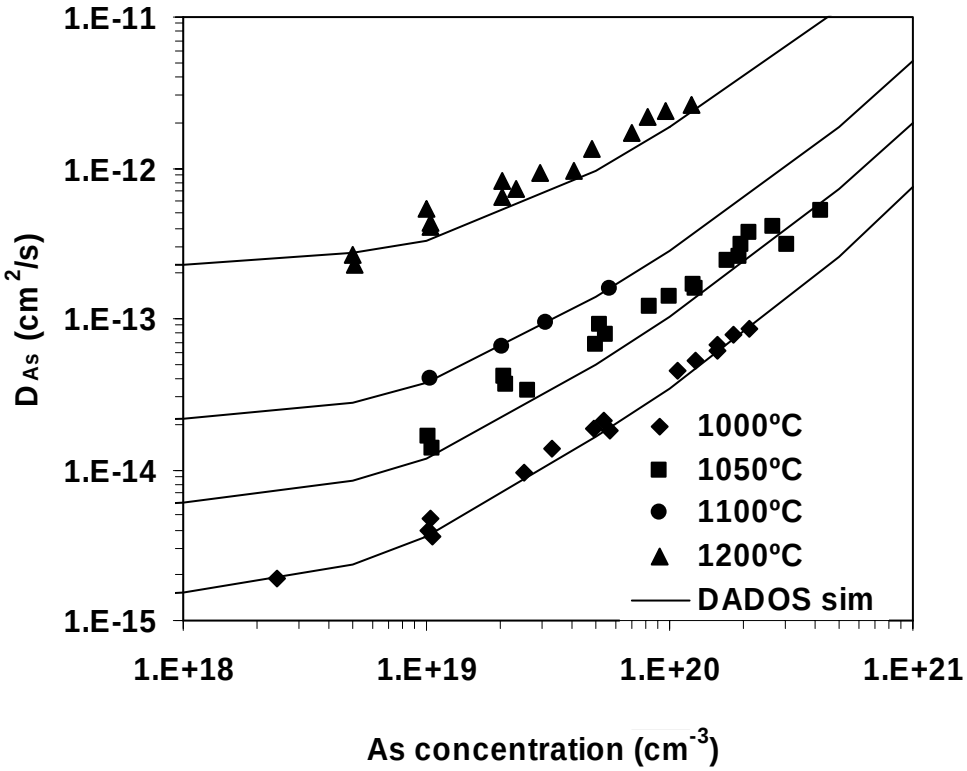
1.E-11
1.E-12
1.E-13
1.E-14
1.E-15
D As (cm 2/s)
1.E+18
1.E+19
1.E+20
1.E+21
As concentration (cm-3)
1000ºC
1050ºC
1100ºC
1200ºC
DADOS sim

Figure 1

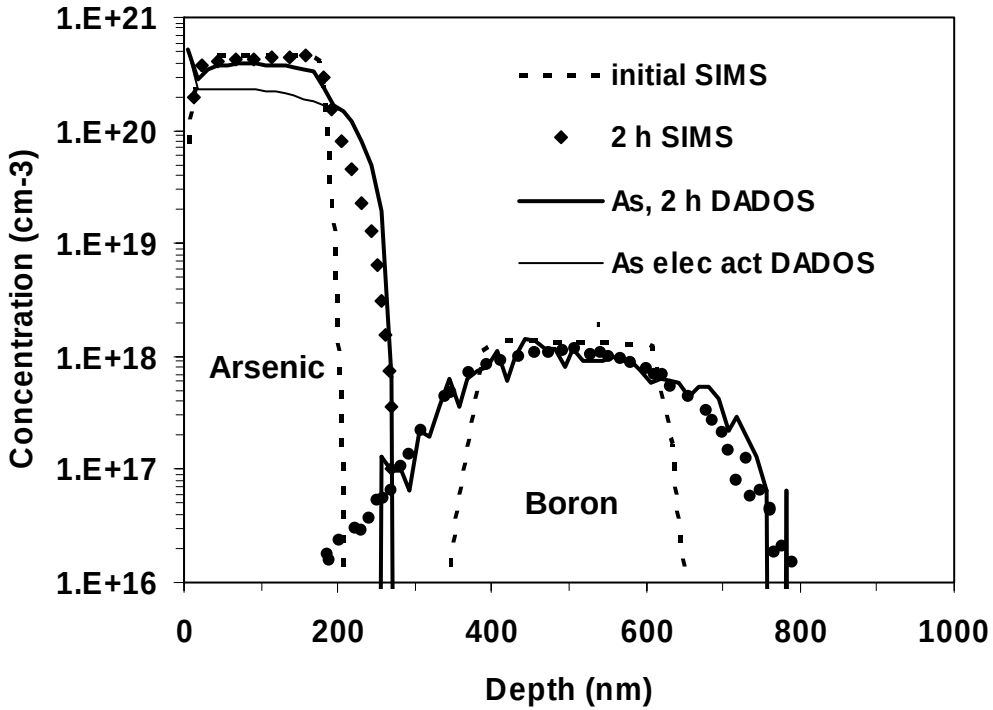
1.E+21
1.E+20
1.E+19
1.E+18
1.E+17
1.E+16
Concentration (cm-3)
initial SIMS
2 h SIMS
As, 2 h DADOS
As elec act DADOS
Arsenic
Boron
0
200
400
600
800
1000
Depth (nm)

Figure 2

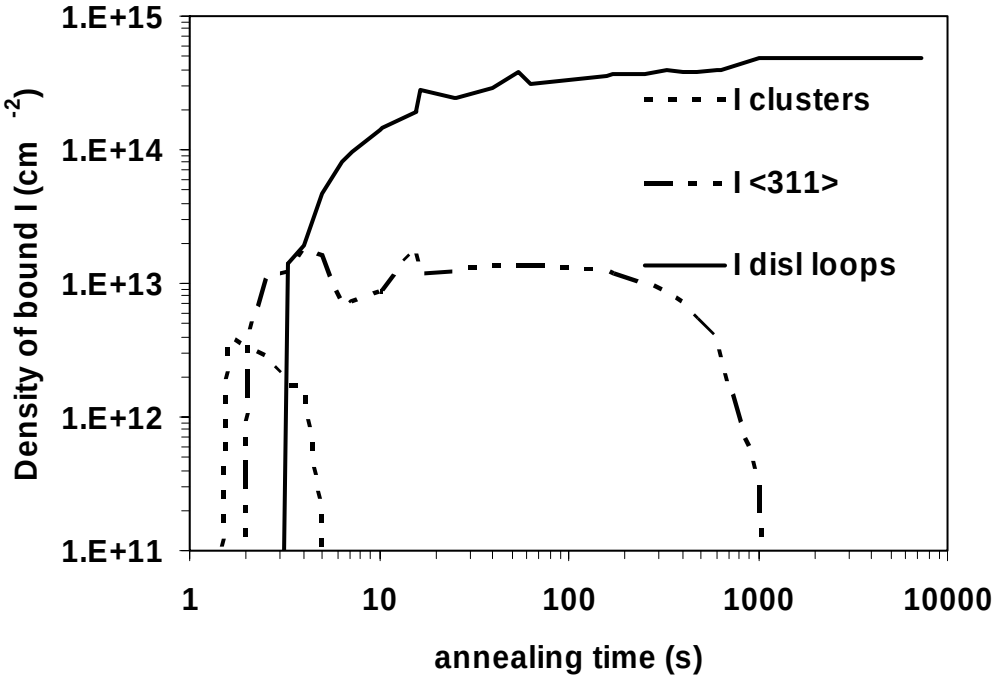
1.E+15
1.E+14
1.E+13
1.E+12
1.E+11
Density of bound I (cm -2)
1
10
100
1000
10000
annealing time (s)
I clusters
I <311>
I disl loops

Figure 3

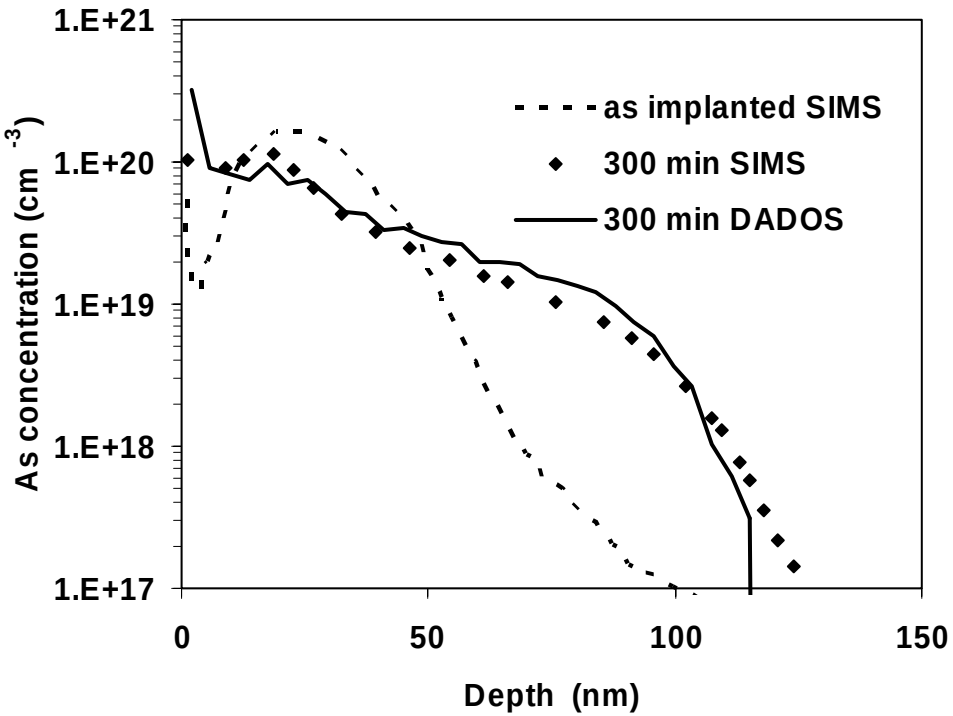
1.E+21
1.E+20
1.E+19
1.E+18
1.E+17
As concentration (cm -3)
0
50
100
150
Depth (nm)
as implanted SIMS
300 min SIMS
300 min DADOS

Figure 4a)

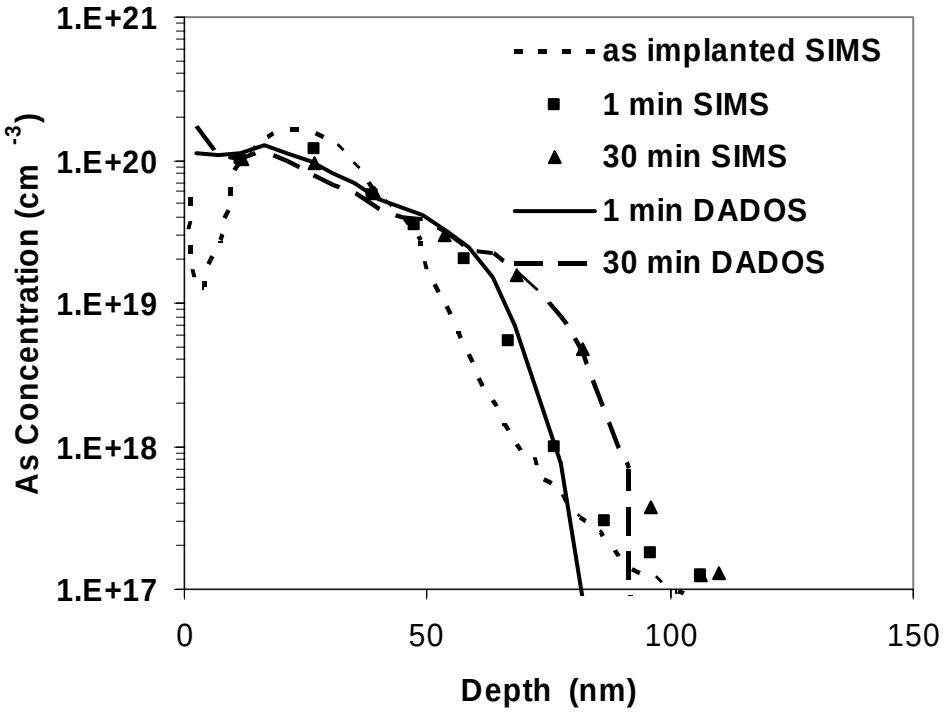
1.E+21
1.E+20
1.E+19
1.E+18
1.E+17
As Concentration (cm -3)
0
50
100
150
Depth (nm)
as implanted SIMS
1 min SIMS
30 min SIMS
1 min DADOS
30 min DADOS

Figure 4b)

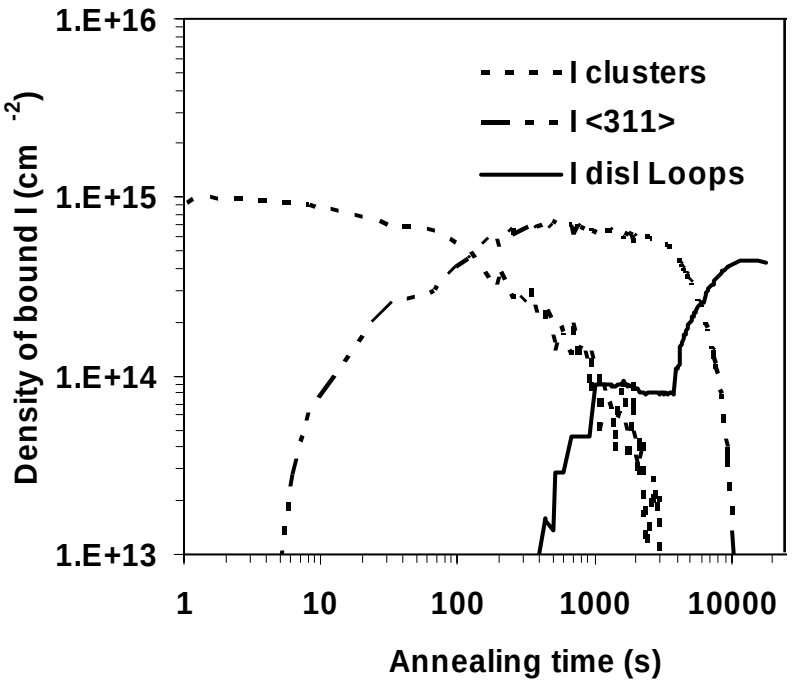
1.E+16
1.E+15
1.E+14
1.E+13
Density of bound I (cm -2)
I clusters
I <311>
I disl Loops
1
10
100
1000
10000
Annealing time (s)

Figure 5

1 P. M. Fahey, P. B. Griffin, J. D. Plummer, Rev. Mod. Phys. 61 (1989) 289

2 P. M. Rousseau, P. B. Griffin, W. T. Fang, J. D. Plummer, J. Appl. Phys. 84 (1998) 3593

3 D. Nobili, S. Solmi, J. Shao, J. Appl. Phys. 90 (2001) 101

4 M. Jaraiz, P. Castrillo, R. Pinacho, I. Martin-Bragado, J. Barbolla, in Simulation of Semiconductor Processes and Devices 2001, edited by D. Tsoukalas and C. Tsamis (Simulation of semiconductor processes and devices, SISPAD, Viena, 2001) pp. 10

5 J. E. Rubio, M. Jaraiz, I. Martin-Bragado, R. Pinacho, P. Castrillo, J. Barbolla, presented at the Spring meeting E-MRS 2004 (symposium B)

6 S. Matsumoto, Y. Ishikawa, T. Niimi J. Appl. Phys. 54 (1983) 5049

7 R. B. Fair in Impurity Doping, Chapt 7,edited by F. F. Y. Wang, North-Holland Publishing Company 1981, p. 315

8 M. Ramamoorthy, S: T. Pantelides, Phys. Rev. Lett., 76 (1996) 4753

9 S. A. Centoni, B. Sadigh, G. H. Gilmer, M-J Caturla, T. J. Lenosky, T. Díaz de la Rubia, C. B. Musgrave, APS/123-QED

10 C. S. Nichols, C. G. Van de Walle, S. T. Pantelides, Phys. Rev. Lett. 62 (1989) 1049

11 Taurus Reference Manual, version 2001.4, Avant! Corp. Fremont, USA

12 I. Martin-Bragado, R. Pinacho, P. Castrillo, M. Jaraiz, J. E. Rubio, J. Barbolla, presented at the Spring meeting E-MRS 2004 (symposium B)

13 D. Nobili, S. Solmi, A. Parisini, M. Derdour, A. Armigliato, L. Moro, Phys. Rev. B 49 (1994) 2477

14 S. Solmi, D. Nobili, J. Appl. Phys. 83 (1998) 2484

15 D.C. Mueller, E: Alonso, W. Fichtner, Phys. Rev. B, 68 (2003) 045208

16 K. C. Pandey, A. Erbil, G. S. Cargill, R. F. Boehme, Phys. Rev. Lett. (1988) 1282

17 M. A. Berding, A. Sher, M. Van Schilfgaarde, P. M. Rousseau, W. E. Spicer, Appl. Phys. Lett. 72 (1998) 1492

18 D. J. Chadi, P. H. Citrin, D. L. Adler, M. A. Marcus, H. J. Gossmann, Phys. Rev. B 49, 2477 (1994)

19 V. Ranki, J. Nissilä, K. Saarinen, Phys. Rev. Lett., 88 (2002) 105506

20 D. W. Lawther, U. Myler, P.J. Simpson, P. M. Rousseau, P. B. Griffin, J. D. Plummer Appl. Phys. Lett. 67 (1995) 3575

21 T. Dunham, P. Fastenko, Z. Qin, M. Diebel, IEICE Trans. Electron., Vol. E86-C, (2003) 276

22 O. Dokumaci, P. Rousseau, S. Luning, V. Krishnammorthy, K. S. Jones, M. E. Law, J. Appl. Phys. 78 (1995) 828

23 R: Kim, T. Auki, Y. Furuta, H. Kobyashi, J. Xia, T. Saito, Y. Kamakkura, K. Taniguchi, Mater. Res. Soc. Symp. Proc 610, (2000) B8.2.1.